

Towards Routine Automated Error Assessment in Antenna Spherical Near-Field Measurements

Patrick Pelland[#], Jonathan Ethier[#], Daniël Janse van Rensburg⁺, Derek McNamara[#], Leili Shafai^{*}, Shantnu Mishra^{*}

[#]SITE, University of Ottawa, Ottawa, Ontario K1N 6N5, Canada
ppell050@uottawa.ca, jethi061@uottawa.ca, mcnamara@site.uottawa.ca

⁺Nearfield Systems Inc., Torrance, CA 90502-1104, USA,
drensbu@nearfield.com

^{*}DFL, Canadian Space Agency, Kanata, Ontario K2H8S2, Canada
leili.shafai@asc-csa.gc.ca, shantnu.mishra@asc-csa.gc.ca

Abstract — This paper describes a measurement process that permits an assessment of spherical near-field (SNF) measurement errors based on a set of tests that can be done as part of any SNF measurement. A test system has been implemented that, in an automated fashion, derives error bars for the measured radiation patterns.

I. INTRODUCTION

This paper describes a new measurement process that will permit an assessment of spherical near-field (SNF) measurement errors based on a set of tests that can be done as part of any SNF measurement. The purpose is to achieve a test system that would, in an automated fashion, derive error bars for a measured radiation pattern. To properly relate the work presented here to that existing in the open literature, a thorough review of this material is required.

A number of papers have been written on the numerous error contributions in SNF antenna measurements. Reference [1] discusses the simulation of mechanical and electrical errors (ten term) associated with SNF measurements. Provision for chamber reflections and equipment-related uncertainty can be added to the analysis, but requires experimental rather than simulation data. A discussion on the alignment of spherical near-field rotators using electrical measurements is discussed in [2]. It shows how it is impractical to use mirrors for AUT alignment. An alternative is to perform repeated measurements of the AUT and use these results to improve alignment with each new measurement. Reference [3] discusses some methods on how one can estimate the error associated with several antenna parameters. The authors of [3] utilize six alignment error quantities, as opposed to the ten introduced in [1]. An interesting plot is [3, Fig. 3] which shows the measured error signal level. Reference [4] presents a discussion of discrepancy in the literature where two papers showed conflicting conclusions regarding error in SNF measurement. The conclusion was theta-scans that pass through the poles (which use phi-scans of 180 degrees) produce phase errors in a plus and minus sense that tend to cancel in the on-axis direction. On the other hand, theta-scans that do not pass through the poles (which use phi-scans of 360 degrees) do not have this canceling effect. Hence, the geometry of

measurement is critical in reducing errors in SNF measurements. An exhaustive error budget is proposed in [5], where an attempt is made to mimic the 18-term error budget associated with planar near-field (PNF) measurements as originally proposed by the National Institute of Standards Technology (NIST) in the USA. The authors of [5] propose a 30-term error budget principally to obtain a qualitative understanding of the entire problem, and so do not provide quantitative verification through measurement or simulation. Reference [6] concentrates on the measurement uncertainties due to probe theta/phi position errors. The authors point out that previous to [6] there was a reliance on the results of PNF uncertainty guidelines to predict SNF uncertainties, in the sense that minimum probe position errors are specified to keep error quantities below acceptable thresholds. Hence, they derive more specific expressions (algorithms if you will) for these probe position errors. They use a simulation approach, quite similar to [1], and quote measurement uncertainties for some standard antennas. A 20-term error budget is proposed in [7]. The approach is theoretical, its authors intending it to be of a “foundational” nature that future authors could use as a basis. The same authors consider more specific estimates of measurement error in the near-field, and their effects on the far-field, in a follow up paper [8]. Reference [9] discusses the use of self-comparison testing in SNF measurements. It uses an over-determined set of measurements which helps to qualify various near-field related sources of error including positioner alignment, chamber reflections and errors introduced by truncation. They use an eight-step process that identifies errors and repeats the measurement to correct for these errors. A theoretical examination at the effects of reflections in SNF chambers is considered in [10], which proposes measuring the near-field over two spheres, separated by a quarter-wavelength. Reference [11] discusses a method to characterize the performance of SNF chambers, and establishes an 18-term error budget along the same lines as the NIST 18-term error budget for PNF systems. The errors can be determined using the tests proposed in [11]. Reference [12] discusses the use of two sets of measurements from two different chambers, and compares the uncertainty to validate conventional assumptions. The estimation of measurement error due to the imperfect polarization properties of probes is

discussed in [13] for all three conventional types of near-field measurements, including SNF. Finally, [14] describes an algorithm that can be used to assess SNF chamber performance.

II. ERROR ASSESSMENT STEPS & ORDERING

We are here interested in an approach that will permit an assessment of SNF measurement error based on a set of practical tests that can be done on a routine basis. The assessment must provide reasonable engineering estimates of the error in the quantities being measured. The review of the literature on techniques that have been used to assess SNF measurement errors has clarified the details of the N-term budgets that have been used by various authors. This has allowed us to identify a list of specific sets of measurements that can be carried out automatically on both an AUT and the test set-up, and used to evaluate the error terms. We adapt the 18-term error budget originally devised by NIST for PNF measurements, and more recently adapted to SNF measurements [11]. This is summarised in Table I and II. A list of the SNF measurements required to quantify the uncertainty associated with each error term is given in Table III. Lastly, some of the terminology used in the above tables is clarified in Table IV.

The goal is to provide a measure of the uncertainty in a particular radiation pattern. We therefore need to understand the relationship between an error term and its associated measurement uncertainty. The various sources of uncertainty outlined in Tables I and II can be broadly classified as (a) uncertainties provided by manufacturer quoted specifications, and (b) uncertainties obtained using measurements done on the SNF test range itself. In order to calculate the measurement uncertainty in case (b) we require measurements M1 through M6 (except for M5) listed in Table III. These provide amplitude radiation patterns $A_i(\theta, \phi)$ at (θ, ϕ) for $i = 1, 2, 3, 4$ and 6. Pattern $A_1(\theta, \phi)$ is considered to be the nominal pattern (the “quoted measurement data”), which we will denote by $S(\theta, \phi)$. The error signal level is defined as the difference in amplitudes of two otherwise (in the ideal case) identical radiation patterns

$$E_{error}(\theta, \phi) = |A_i(\theta, \phi) - A_j(\theta, \phi)| \quad (1)$$

Next, one determines the error-to-signal ratio with respect to the amplitude of the quoted measurement data as (in dB)

$$E_{error}(\theta, \phi) / S(\theta, \phi) = \left\{ E_{error}^{dB}(\theta, \phi) - S^{dB}(\theta, \phi) \right\} \quad (2)$$

Lastly, the measurement uncertainty associated with that particular error-to-signal ratio can be found as

$$U(\theta, \phi) = \pm 20 \log \left(1 - 10^{\frac{E_{error}(\theta, \phi) / S(\theta, \phi)}{20}} \right) \quad (3)$$

Once all uncertainties have been determined, they are added together using the root sum of squares method (RSS). Figure 1 shows a sample output radiation pattern with upper and lower bounds due to uncertainty.

As outlined in Table III, a total of six SNF scans must be taken in order to quantify measurement uncertainties for all non-manufacturer related error terms. First the “quoted radiation pattern” is acquired using the redundant sphere measurement M₁. This will result in two field values at every measurement point. Since each data subset (180-phi & 360-phi) contains its own unique alignment errors, the averaging of the two yields a more accurate measurement [11]. After the redundant sphere scan, five additional measurements (M2, M3, M4, M5 and M6) are taken, each serving to quantify one or more uncertainties, as outlined in Tables I and II.

TABLE I
FIRST HALF OF THE 18-TERM ERROR BUDGET & MEASUREMENT

#	Error Term	Description	Test Procedure
1	Probe Relative Pattern	Error introduced by imperfect probe correction model.	Compare probe corrected M1 to off-band probe corrected M1.
2	Probe Polarization	Error introduced by probe's non-zero cross-polarization level.	From manufacturer information, apply uncertainty to M1.
3	Probe Gain	Contribution due to uncertainty in probe gain.	From manufacturer information, apply uncertainty to M1.
4	Probe Alignment	Uncertainty due to probe alignment errors.	<i>See Error Term #1</i>
5	Normalization Constant	Measurement uncertainty introduced by attenuator.	From manufacturer information, apply uncertainty to M1.
6	Impedance Mismatch	The uncertainty in measured input reflection of AUT/probe.	From manufacturer information, apply uncertainty to M1.
7	AUT Alignment Error	Uncertainty introduced due to imperfect AUT alignment.	Perform AUT mechanical alignment and note uncertainty.
8	Data Spacing	Error introduced by finite number of sample points.	Compare M5 to regular density subset of M5.
9	Data Truncation	Error introduced by using partial sphere data.	Perform NF - FF transformation on M1 using finite region window.

The order in which the required measurements are performed is shown in Table V. The identifier [TABLEnn] denotes that data is saved into a lookup table for the particular step and is AUT-independent. Steps marked [USERnn] and [AUTOnn] are not AUT-independent. The identifier [USERnn] means that user intervention is required. Lastly, identifier [AUTOnn] means that the test is performed automatically by

the acquisition code developed to automate the error assessment process. The order has been devised to minimize the overall time to complete an error assessment. The correct order is especially important to permit resumption of data set acquisition should any single step prove to be temporarily problematic.

III. SOME PRACTICALITIES

One should expect measurement uncertainty to increase as one deviates further and further from the AUT's main beam. As the signal amplitude decreases, the error-to-signal ratio will increase. One can expect a similar behaviour in a cross-polarization measurement, where the signal amplitude tends to be considerably lower than the main beam's amplitude.

The use of a dual-polarized probe is avoided here as the variation in electrical path length between the probe's ports tends to increase measurement uncertainty. While one can create a detailed, frequency dependent normalization database to account for this variation, these will only correct the problem with its own associated uncertainty. Setups employing a dual-polarized probe should add its associated uncertainty to the error budget as a new term or packaged with error term #2.

In order to determine the measurement uncertainty associated with probe/AUT reactive coupling, the radius of the measurement sphere is increased by $\lambda/4$ and re-measured (M6). By comparing the data from two spheres with radii differing by $\lambda/4$, one expects identical normalized radiation patterns. However, unwanted probe/AUT interactions due to multiple reflections give rise to a difference between the signals from the two scans (and "error signal"). Care should be taken when manually moving the AUT along the z-axis as additional alignment errors tend to arise. On the other hand, any error associated with probe alignment, however small, is included in the estimation of error term #1 [11]. Therefore, one should ideally move the probe rather than the AUT unless the SNF setup has the ability to accurately translate the AUT along the z-axis.

IV. RELATIVE IMPORTANCE OF THE ERROR ASSESSMENT DATA SETS

Error term #9 provides a measure of uncertainty arising from using an open measurement window rather than a closed surface (sphere). Ironically, one must make a full sphere measurement to determine the error associated with data truncation. While this term provides a useful reference for the effects of truncation in a particular setup, it may be bypassed and listed as "not applicable" should one have no interest in truncating the measurement sphere.

Error term #18 is associated with the system's repeatability and random errors. Ideally, identical scans should yield no error signal level. In practice, random errors will always have an impact on a measured radiation pattern. In a typical setup, the uncertainty associated with random errors and repeatability should be minor. If this error term tends to be

larger than expected, one should investigate in an attempt to identify/remedy the cause.

Error term #16 attempts to quantify the uncertainty associated with chamber reflections. The AUT points in different directions within the chamber when a 180-phi scan is carried out than when a 360-phi scan is executed. The difference between the two patterns can be attributed principally to anechoic chamber absorber performance. However, this difference will also be partly due to AUT alignment errors, as each scan employs a different AUT rotation scheme. By performing an accurate AUT alignment, and noting the alignment uncertainty prior to the measurement process, one can minimize the AUT's misalignment contributions to error term #16.

TABLE II
SECOND HALF OF THE 18-TERM ERROR BUDGET & MEASUREMENT

M	Error Term	Description	Measurement
10	XY Position Errors	See Error Term #11	See Error Term #11
11	Z Position Errors	Error introduced by position errors (imperfect sphere).	Compare regular density subset of M5 to M1.
12	Probe / AUT Multiple Reflections	Error introduced by unwanted probe and AUT interactions.	Compare M6 ($\lambda/4$ -larger sphere) to regular density subset of M5.
13	Receiver Amplitude Linearity	Error caused by non-linear amplitude response of receiver.	Apply manufacturer specified non-linearity profile to M1.
14	System Phase Error	Error caused by variable electrical path length due to imperfect rotary joints.	Note the peak-to-peak field variation in M5.
15	Receiver Dynamic Range	Error caused by RF sub-system limited dynamic range.	The on-axis SNR from M3.
16	Room Scattering	Error introduced by scattering due to imperfect chamber.	Comparison between 180-phi and 360-phi data subsets of M1.
17	Cable Leakage	Error introduced by unwanted radiation.	Measure pattern due to terminated cable and apply uncertainty to M1.
18	Repeatability & Random Errors	Errors associated with repeatability.	Compare identical measurements M3 and M4.

A setup employing this measurement process will find that it may be impractical to run all required tests on a routine basis, since it may require many hours to complete. Therefore, a detailed database of all uncertainties for various AUT categories can be created for a particular SNF setup. One might also discover that certain error terms are chamber/setup specific and do not depend on the AUT. They could thus be re-used if appropriate. This can significantly reduce chamber

occupancy while still providing reasonable estimates of uncertainty.

TABLE III
MEASUREMENT NUMBERING & DETAILS

M	Scan Geometry	Details
1	Double Sphere	Measurement taken at slow scan speed. The averaged double sphere is the quoted measurement data.
2	180-Phi	Measurement taken using double density samples.
3	360-Phi	Record the SNR of the on-axis field measurement.
4	360-Phi	Used for repeatability assessment.
5	-	Rotate the AUT's phi axis and probe axis simultaneously, note the field variation.
6	180-Phi	Measurement taken using a $\lambda/4$ larger sphere than all previous measurements.

TABLE IV
TERMINOLOGY USED IN THE DESCRIPTION OF THE MEASUREMENTS USED TO ACQUIRE DATA FOR UNCERTAINTY ESTIMATION

Terminology	Description
180-phi Scan	Measurement sphere acquired with AUT rotation of $0 \leq \Phi \leq 180^\circ, -180^\circ \leq \theta \leq 180^\circ$.
360-phi Scan	Measurement sphere acquired with AUT rotation of $0 \leq \Phi \leq 360^\circ, 0 \leq \theta \leq 180^\circ$.
Redundant/Double Sphere	Measurement sphere acquired with $0 \leq \Phi \leq 360^\circ, -180^\circ \leq \theta \leq 180^\circ$. When averaged, this becomes the "quoted measurement" data. 180-phi and 360-phi data subsets can also be extracted.

TABLE V
SECOND HALF OF THE 18-TERM ERROR BUDGET & MEASUREMENT

[TABLE 01]: Create a lookup table that contains information on various chamber/setup related uncertainties.
[TABLE 02]: Update lookup table to reflect setup changes.
[TABLE 03]: Terminate cable feeding AUT and measure cable's radiation/leakage pattern. Data is saved in table as T1.
[TABLE 04]: Record uncertainties relating to error terms #2, #3, #5, #6, #13. Data is saved in the table as T2, T3, T4, T5 and T6, respectively.
[USER 01]: Mount the AUT and estimate AUT alignment uncertainty. Data is saved in the table as T7.
[USER 02]: Run the automated error assessment script.
[AUTO 01]: Acquire M1.
[AUTO 02]: Acquire M2.
[AUTO 03]: Acquire M3.
[AUTO 04]: Acquire M4.
[AUTO 05]: Acquire M5.
[USER 08]: Increase the size of the measurement sphere by $\lambda/4$.
[AUTO 06]: Acquire M6.
[AUTO 07]: Process uncertainty budget based on completed measurements.
[AUTO 08]: Output radiation patterns with error bars.

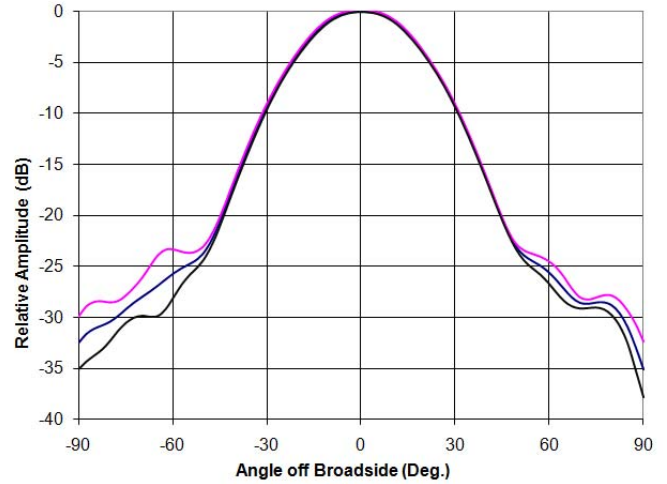


Fig. 1 A sample radiation pattern output showing upper bounds (—) and lower bounds (—) determined from the uncertainty obtained using the procedure described.

V. CONCLUSIONS

This paper describes an automated process that permits an assessment of spherical near-field (SNF) measurement errors based on a set of practical tests that can be done as part of any SNF measurement. A test system has been implemented that, in an automated fashion, derives error bars for the measured radiation patterns. The method also serves as a useful tool for routine chamber maintenance.

REFERENCES

- [1] D.J Janse van Rensburg, S. Mishra, G. Seguin, "Simulation of Errors in Near-Field Facilities", Proc. Antenna Measurement Techniques Association (AMTA) Annual Symp., pp. 336 – 340, 1995.
- [2] A. Newell, G. Hindman, "The Alignment of a Spherical Near-Field Rotator using Electrical Measurements", Proc. Antenna Measurement Techniques Association (AMTA) Annual Symp., pp. 131 – 136, 1997.
- [3] A. Newell, G. Hindman, "Quantifying the Effect of Position Errors in Spherical Near-Field Measurements", Proc. Antenna Measurement Techniques Association (AMTA) Annual Symp., pp. 145 – 149, 1998.
- [4] A. Newell, G. Hindman, "The Effect of Measurement Geometry on Alignment Errors in Spherical Near-Field Measurements", Proc. Antenna Measurement Techniques Association (AMTA) Annual Symp., pp. 274 – 279, 1999.
- [5] D. Hess, "An Expanded Approach to Spherical Near-Field Uncertainty Analysis", Proc. Antenna Measurement Techniques Association (AMTA) Annual Symp., 2002.
- [6] A. Newell, "Estimating the Uncertainties due to Position Errors in Spherical Near-Field Measurements", Proc. Antenna Measurement Techniques Association (AMTA) Annual Symp., 2003.
- [7] M. Francis, R. Wittmann, "Uncertainty Analysis for Spherical Near-Field Measurements", Proc. Antenna Measurement Techniques Association (AMTA) Annual Symp., 2003.
- [8] R. Wittmann, M. Francis, "Spherical-Scanning Measurements: Propagating Errors through the Near- to Far-Field Transformation", Proc. Antenna Measurement Techniques Association (AMTA) Annual Symp., 2004.
- [9] G. Hindman, A. Newell, "Spherical Near-Field Self-Comparison Measurements", Proc. Antenna Measurement Techniques Association (AMTA) Annual Symp., 2004.
- [10] M. Francis, J. Guerrieri, Katie MacReynolds, R. Wittmann, "Estimating Multiple-Reflection Uncertainties in Spherical Near-Field

- Measurements”, Proc. Antenna Measurement Techniques Association Proceedings (*AMTA*) Annual Symp., 2004.
- [11] G. Hindman, A. Newell, “Simplified Spherical Near-Field Accuracy Assessment”, Proc. Antenna Measurement Techniques Association (*AMTA*) Annual Symp., 2006.
- [12] A. Newell, G. Hindman, “Planar and Spherical Near-Field Range Comparison with -60 dB Residual Error Level”, Proc. Antenna Measurement Techniques Association (*AMTA*) Annual Symp., 2007.
- [13] A. Newell, “Cross Polarization Uncertainty in Near-Field Probe Correction”, Proc. Antenna Measurement Techniques Association (*AMTA*) Annual Symp., 2008.
- [14] G. Hindman, A. Newell, “Mathematical Absorber Reflection Suppression (MARS) for Anechoic Chamber Evaluation and Improvement”, Proc. Antenna Measurement Techniques Association (*AMTA*) Annual Symp., 2008.